Pharmaceutical Sciences and Drug Design
ISSN: 3062-4428
2022, Volume 2, Page No: 101-116

Available online at: www.galaxypub.co/page/journals

Galaxy Publication

Galaxy Publication

Inhibition of cGAS/STING-Mediated Cellular Senescence Underlies the Protective Effect of Ginsenoside Rg1 in Experimental Pulmonary Hypertension

Klara Novak[1]*, Andrei Benes[1]

[1]Department of Biotechnology, Faculty of Natural Sciences, Charles University, Prague, Czech Republic.

***E-mail** ✉ klara.n.cz@outlook.com

Received: 28 November 2021; **Revised:** 15 February 2022; **Accepted:** 18 February 2022

ABSTRACT

Pulmonary hypertension (PH) is a life-threatening disease of the pulmonary vasculature for which effective therapeutic options remain scarce. Although ginsenoside Rg1 has shown beneficial activity in alleviating PH, the molecular basis of its action has not been fully clarified. This work aimed to elucidate the signaling mechanisms through which ginsenoside Rg1 improves PH. A rat model of PH was used to evaluate the therapeutic impact of ginsenoside Rg1 via cardiopulmonary hemodynamic analysis and tissue staining. Network-pharmacology approaches were applied to predict possible molecular targets, and immunofluorescence was used to assess protein expression within the cyclic GMP–AMP synthase (cGAS)/stimulator of interferon genes (STING) axis. Transcriptional and protein levels of senescence indicators were measured using RT-PCR and immunohistochemistry, and ELISA was performed to detect senescence-associated secretory phenotype (SASP) molecules.

Ginsenoside Rg1 markedly reduced right ventricular systolic pressure (RVSP). Echocardiographic analysis showed increased pulmonary artery acceleration time/pulmonary ejection time (PAT/PET) and enhanced tricuspid annular plane systolic excursion (TAPSE), along with a decrease in right ventricular anterior wall thickness (RVAWT). Hematoxylin–eosin staining demonstrated substantial attenuation of pulmonary vascular remodeling. In addition, Rg1 significantly suppressed mRNA and protein levels of senescence markers p21 and p16, and sharply lowered NF-κB, IL-6, and IL-8. These findings support that ginsenoside Rg1 mitigates pulmonary vascular remodeling in PH, potentially through inhibiting cellular senescence via the cGAS/STING pathway.

Keywords: Ginsenoside Rg1, Pulmonary hypertension, cGAS/STING pathway, Cellular senescence, Pulmonary vascular remodeling

How to Cite This Article: Novak K, Benes A. Inhibition of cGAS/STING-Mediated Cellular Senescence Underlies the Protective Effect of Ginsenoside Rg1 in Experimental Pulmonary Hypertension. Pharm Sci Drug Des. 2022;2:101-16. https://doi.org/10.51847/tEoQeHsnVz

Introduction

Pulmonary hypertension (PH) is a debilitating cardiopulmonary disorder that threatens human health worldwide, affecting roughly 1% of the population and nearly 10% of individuals aged 65 years and above [1]. A defining feature of PH is irreversible pulmonary vascular remodeling (PVR) [2]. The disease is characterized by thickened distal pulmonary arterioles and progressive luminal narrowing, which elevate pulmonary vascular resistance and arterial pressure, subsequently provoking right ventricular hypertrophy and, eventually, right-sided heart failure [3, 4]. Although substantial progress has been made toward understanding PH, the multifaceted nature of the disease continues to hinder the development of effective therapies, leaving mortality rates high [5, 6]. Clarifying disease mechanisms and finding improved treatment strategies remain urgent needs.

Cellular senescence refers to a lasting arrest of cellular proliferation, typically induced by telomere deterioration, oxidative stress, or genomic injury [7]. Senescence generally arises in two forms: replicative senescence and stress-induced premature senescence [8]. Replicative senescence results from progressive telomere loss and the subsequent activation of DNA-damage signaling pathways [9]. By contrast, stress-related premature senescence is triggered by external insults—such as oxidative molecules or radiation—that force cells into a senescent state

earlier than expected [10, 11]. Despite sharing similar phenotypic and molecular traits, premature senescence occurs independently of telomere length [12].

Senescence is increasingly recognized as a crucial contributor to PH. Pulmonary artery smooth muscle cells (PASMCs), which make up the medial layer of pulmonary vessels, can undergo senescence upon exposure to environmental stresses, including particulate pollutants, cigarette smoke, hypoxia, and inflammatory mediators [13, 14]. The senescence-associated secretory phenotype (SASP) comprises a broad range of secreted cytokines, chemokines, proteases, and growth factors produced by senescent cells [15]. Senescent PASMCs influence PH progression by altering cell-cycle regulation and, through SASP factors, modifying the survival, proliferation, and migratory behavior of both senescent and adjacent non-senescent cells [16].

The cGMP–AMP synthase (cGAS)/STING pathway is a key sensor in innate immunity, detecting abnormal nucleic acids present in the cytoplasm [17]. Upon recognizing mitochondrial DNA (mtDNA) released from damaged mitochondria, cGAS activates STING, which then triggers a cascade of downstream signaling events that regulate diverse cellular processes [18]. Recent studies highlight that this pathway plays significant roles in cardiovascular disorders, aging, and cancer [19–21]. In pulmonary artery smooth muscle cells (PASMCs), mitochondrial injury releases superoxide and mtDNA, activating the cGAS/STING/NF-κB axis and thereby facilitating PH development [22]. Targeting this signaling pathway can suppress PASMC proliferation and phenotype switching, offering a promising therapeutic strategy for PH [23]. Nevertheless, the precise mechanisms by which cGAS/STING contributes to PASMC senescence in PH remain to be elucidated.

Panax ginseng C.A. Meyer, a perennial member of the Araliaceae family, has been used in traditional Chinese medicine for centuries [24, 25]. Modern pharmacology identifies ginsenosides as its principal bioactive compounds, with Rg1 being the most extensively investigated due to its anti-inflammatory, anti-aging, and anti-cancer properties [26–28] In mouse models of sepsis-induced myocardial injury, Rg1 activates the FAK/AKT–FOXO3A pathway, reducing cardiomyocyte apoptosis, inflammation, and iron deposition [29]. In rat models of cardiac arrest and cardiopulmonary resuscitation, Rg1 protects cognitive function by restoring synaptic integrity and activity [30]. It further diminishes oxidative stress, lowers apoptosis, enhances antioxidant enzyme activity, and slows cellular aging [31]. Additionally, Rg1 promotes autophagy and mitigates paraquat-induced pulmonary fibrosis by upregulating ATG12, which concurrently reduces senescence and SASP [31]. Previous studies also suggest that Rg1 can improve PH by modulating CCN1 expression, reversing hypoxia-induced endothelial-to-mesenchymal transition and inflammatory signaling [32]. In this study, a hypoxia/Sugen-induced PH model was employed to investigate the effects of Rg1 and explore how cGAS/STING-mediated senescence contributes to pulmonary vascular remodeling, providing insights for new PH therapies.

Materials and Methods

Chemicals and antibodies

Rg1 (RS02541020) was sourced from Shanghai Standard Technology Co., Ltd. Sildenafil and Sugen were obtained from Selleck (S1431) and MedChemExpress (HY-10374), respectively. Antibodies against cGAS (PA5-121188), STING (PA5-23381), p-STING (PA5-105674), TBK1 (MA1-20344), p-TBK1 (PA5-105919), p16 (PA5-20379), and p21 (14–6715-81) were purchased from ThermoFisher Scientific. α-SMA (19245) and PCNA (13110) antibodies were obtained from CST.

PH rat model

Male rats, 8 weeks old, were purchased from Hunan SJA Laboratory Animal Co., Ltd. (License CXK (Xiang) 2019–004) and acclimated for 1 week at the Animal Center of Hunan University of Chinese Medicine. PH was induced using combined hypoxia and Sugen injection. Oxygen levels in the chamber were maintained at 10% ±0.5% using N_2 control. Rats were exposed to hypoxia 8 hours/day for 3 weeks, and a single subcutaneous Sugen dose (20 mg/kg/week) was given prior to the hypoxic period. Sample size was calculated (Cohen's $d \approx 1.83$), resulting in $n = 6$ per group for 80% power at $\alpha = 0.05$; $n = 8$ per group was used to compensate for potential attrition. Rats were assigned to six groups: normoxic control (CTR), SuHx model, Rg1 low-dose (10 mg/kg/d, Rg1 L), Rg1 medium-dose (15 mg/kg/d, Rg1 M), Rg1 high-dose (20 mg/kg/d, Rg1 H), and SuHx + Sildenafil (25 mg/kg/d, SIL). Drugs were dissolved in 5% sodium carboxymethyl cellulose and orally administered for 3 weeks. Following treatment, hemodynamic measurements, lung tissues, and serum samples were collected. All

procedures were approved by the Ethics Committee of The First Hospital of Hunan University of Chinese Medicine and adhered to standard laboratory animal care guidelines [33].

Hemodynamic assessment

Right ventricular systolic pressure (RVSP) was measured via external jugular vein catheterization using an MP160 BIOPAC multi-channel system. Rats were anesthetized with isoflurane, and echocardiography was performed to record pulmonary artery acceleration time (PAAT), pulmonary ejection time (PET), tricuspid annular plane systolic excursion (TAPSE), and right ventricular anterior wall thickness (RVAWT).

Hematoxylin–eosin staining

Lung sections were deparaffinized, rehydrated in graded ethanol, and rinsed with distilled water. Sections were stained with hematoxylin for 10 min, differentiated in 1% hydrochloric acid alcohol for 30 sec, washed in water for 15 min, and then stained with eosin. Sections were dehydrated, cleared, and mounted with neutral resin.

Routine blood tests and biochemical detection

Blood was drawn from the abdominal aorta and immediately spun at 1,000 × g for 20 minutes at 4°C to collect serum. Standard hematological values were obtained using a Sysmex XE-2100 automated system (Sysmex Corporation, Kobe, Japan). Serum concentrations of Cr, BUN, AST, and ALT were then quantified on a Hitachi 7600 analyzer (Hitachi Ltd., Tokyo, Japan) according to the instrument protocols.

Target identification and network pharmacology analysis

All work involving open-access human data was approved by the Ethics Committee of The First Hospital of Hunan University of Chinese Medicine. Genes associated with Pulmonary Hypertension were searched in GeneCards and OMIM, then pooled, cleaned of duplicates, and standardized with UniProt. The 2D/3D structure of Ginsenoside Rg1 came from PubChem, and possible human (Homo sapiens) binding targets were forecasted via SwissTargetPrediction and SEA. The overlap between PH-related genes and Rg1-predicted targets was determined using a Venn diagram in Venny 2.1. These shared genes were submitted to STRING with confidence >0.4 for a protein–protein interaction network, which was examined and displayed using Cytoscape 3.9.1. Enrichment (GO and KEGG) was performed with DAVID, applying $p < 0.05$ as the cutoff.

Molecular docking

Protein files were obtained from the RCSB Protein Data Bank as PDB structures. After import into PyMOL, ions and water were deleted. Hydrogens and partial charges were added using AutoDockTools, and proteins were saved as PDBQT. Small compounds taken from PubChem in SDF format were minimized in Chem3D Pro, converted to MOL, and then exported as PDBQT via OpenBabel. Docking simulations were run using AutoDock Vina, with coordinates defined according to the binding pockets in the PDB data.

Wheat germ agglutinin (WGA) staining

Hearts were collected after euthanasia and fixed in 4% paraformaldehyde, then dehydrated through ethanol concentrations from 70% up to 100%. Sections were treated overnight at 4°C with WGA-AF488 solution (W11261, ThermoFisher), followed by DAPI staining for 30 minutes. Slides were mounted and examined using fluorescent microscopy.

Fulton index

Right ventricular remodeling was assessed by Fulton's index, expressed as the ratio RV/(LV + S), comparing the right ventricular weight against that of the left ventricle plus septum.

Immunofluorescence

Lung sections around 4 μm in thickness were deparaffinized, rehydrated, and processed for antigen retrieval. An autofluorescence quencher was added for 5 minutes, then rinsed for 10 minutes, followed by BSA blocking for 30 minutes. Primary antibodies (Anti-PCNA, Anti-α-SMA, Anti-cGAS, and Anti-STING) were applied and left overnight at 4°C. After washing, appropriate secondary antibodies were applied for 50 minutes, nuclei were labeled with DAPI, and the tissue was sealed and visualized microscopically.

Immunohistochemistry staining

Pulmonary tissues underwent antigen retrieval, followed by blocking and suppression of endogenous peroxidase activity at 22–23°C. Primary and secondary antibodies against p16 and p21 were used, after which staining was developed with DAB, and the nuclei were counterstained.

Quantitative real-time PCR (RT-qPCR)

RNA from pulmonary vasculature was extracted using Trizol (15596018CN, ThermoFisher) following the supplied instructions. Reverse transcription and qRT-PCR followed standard protocols.

ELISA

After blood was drawn from the rats' abdominal aorta, the samples were allowed to stand at room temperature for 2 hours, then centrifuged to obtain serum. Diluted serum was pipetted into ELISA plates at 100 μL per well, followed by incubation at 37°C for 90 minutes. A biotin-labeled detection antibody (100 μL) was then added and incubated at the same temperature for 1 hour. Following the wash steps, 100 μL of HRP working solution was applied and kept at 37°C for 30 minutes. Subsequently, 90 μL of the chromogenic substrate was introduced and allowed to react without light exposure for 15 minutes at 37°C. Once the reaction was stopped, absorbance at 450 nm was recorded using a plate reader. Reagents for IL-6 (E-EL-R0015) and NF-κB (E-EL-R0673) were supplied by Elabscience Biotechnology, and IL-8 (ab273236) was purchased from Abcam.

Western blot

Protein extraction and immunoblotting followed published experimental routines. Lung samples were processed in RIPA buffer supplemented with protease and phosphatase inhibitors on ice and centrifuged afterward. The resulting supernatant was assayed for protein concentration using a BCA quantification kit, and 20 μg of protein was electrophoretically separated by SDS–PAGE, then transferred to PVDF membranes. Membranes were blocked and exposed to primary antibodies at 4°C, followed by washes and incubation with HRP-tagged secondary antibodies. Protein signals were visualized using ECL chemistry, imaged, and analyzed in ImageJ, with expression levels standardized to β-actin.

Statistical analysis

Data are expressed as mean ± standard deviation, and all comparisons were performed in GraphPad Prism 10.1.2. A significance threshold of $P < 0.05$ was adopted. Outliers were detected using Grubbs' test. Two-group comparisons were performed using unpaired two-sided Student's t-tests, while experiments involving more than two groups were evaluated with one-way ANOVA, followed by Tukey post hoc tests when needed.

Results and Discussion

Ginsenoside Rg1 improves cardiopulmonary parameters in PH rats

To determine whether Ginsenoside Rg1 influences PH progression, rats received either Ginsenoside Rg1 or Sildenafil by oral administration **(Figures 1a and 1b)**. Animals exposed to hypoxia plus Sugen displayed a pronounced increase in right ventricular systolic pressure (RVSP) compared with healthy controls, confirming a successful PH induction. Treatment with Ginsenoside Rg1 resulted in a dose-responsive decline in RVSP relative to the SuHx model group **(Figures 1c and 1d)**. Echocardiographic assessments showed marked decreases in TAPSE and the PAT/PET ratio in the SuHx animals, whereas Ginsenoside Rg1 significantly mitigated these reductions **(Figures 1e–1h)**. Overall, the data demonstrate that Ginsenoside Rg1 offers measurable protective benefits in this rat model of pulmonary hypertension.

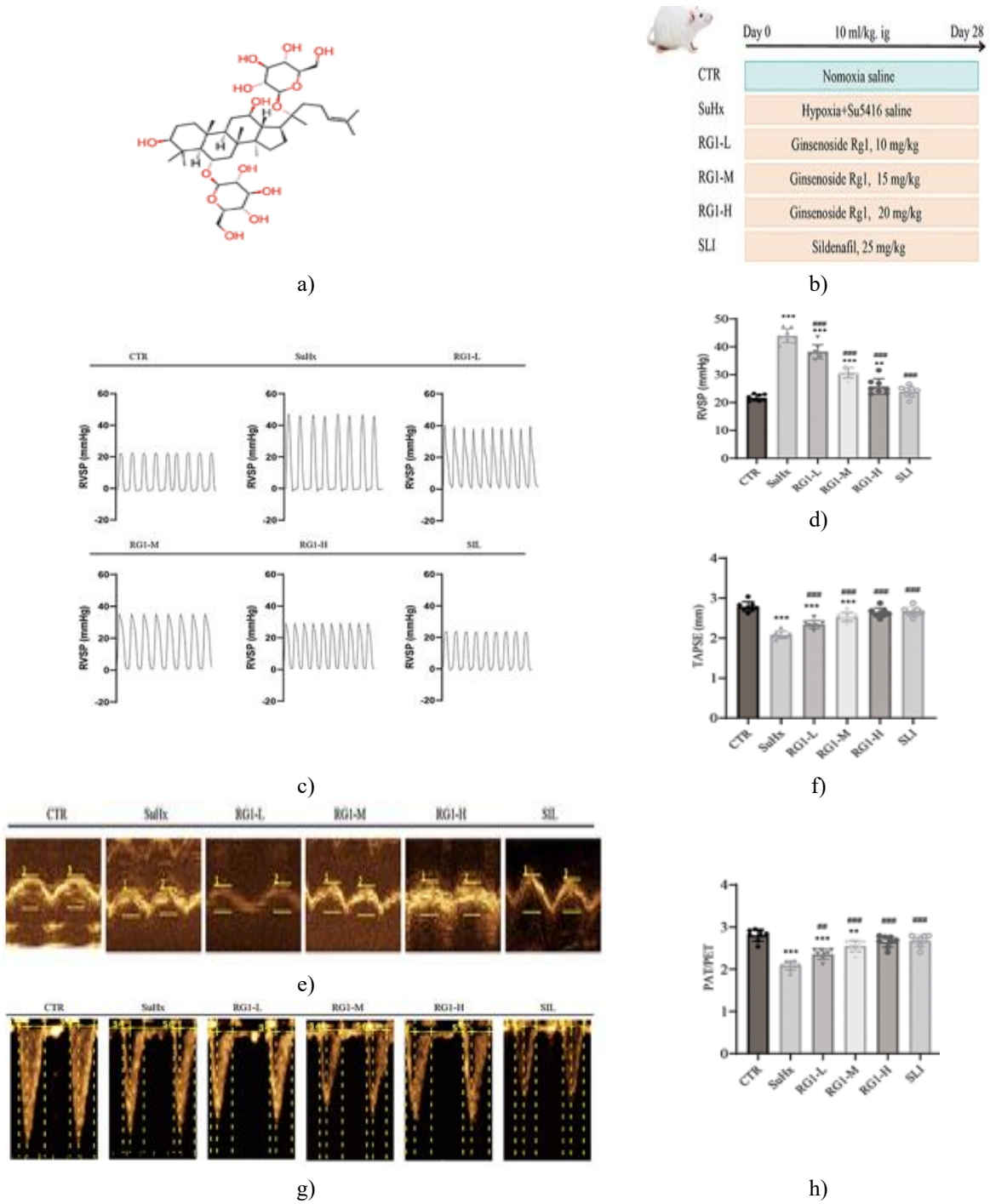

Figure 1. Effects of Ginsenoside Rg1 on Hemodynamics in Su/Hx Rats

(a and b) Rats exposed to Sugen/hypoxia received oral treatments consisting of Sildenafil (25 mg/kg) or Ginsenoside Rg1 at 10, 15, or 20 mg/kg.

(c) Right ventricular systolic pressure (RVSP) was determined via right-heart catheterization across the experimental groups.

(d) Quantitative comparison of RVSP illustrating the impact of Rg1 therapy.

(e) Example echocardiographic images indicating tricuspid annular plane systolic excursion (TAPSE).

(f) Graph charting TAPSE values.

(g) Ultrasound images depicting pulmonary artery acceleration time (PAT) and pulmonary ejection time (PET).

(h) Summary statistics for PAT/PET measurements. Data are presented as mean ± SD, n = 8, analyzed using one-way ANOVA with Tukey's post-test. $P < 0.01$, $P < 0.001$ vs control; ##$P < 0.01$, ###$P < 0.001$ vs Su/Hx.

Ginsenoside Rg1 reduces sugen/hypoxia-driven pulmonary vascular remodeling

Pulmonary arterial remodeling was analyzed by calculating vessel wall thickness percentage (WT%) using HE-stained tissue. Animals subjected to Sugen/hypoxia showed a marked rise in WT% and thickening of the arterial media compared with untreated controls. Administration of Ginsenoside Rg1 significantly reduced these structural changes **(Figures 2a and 2b)**.

To assess smooth muscle cell proliferation in the medial layer, double immunofluorescence was performed using α-SMA (red) and PCNA (green) markers. The SuHx group exhibited strong overlap of α-SMA and PCNA signals, indicating increased PASMC growth. Treatment with Ginsenoside Rg1 weakened this co-localization pattern **(Figures 2c and 2d)**.

Overall, these observations demonstrate that Ginsenoside Rg1 decreases PASMC proliferation and thereby limits the progression of pulmonary vascular remodeling.

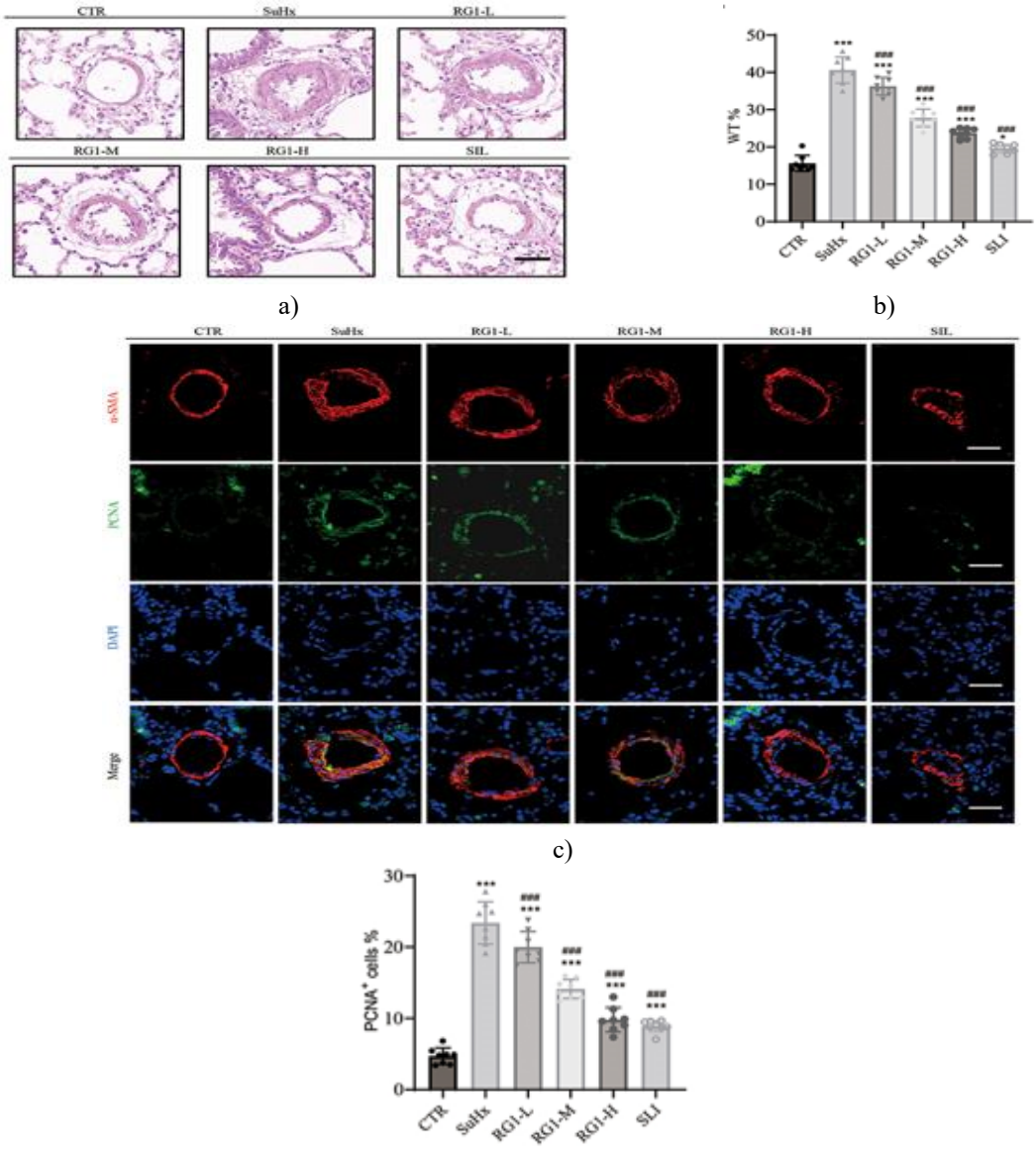

Figure 2. Ginsenoside Rg1 Ameliorates Vascular Pathological Changes

(a) HE-stained lung slices used for assessing arterial medial thickness, scale 50 μm.

(b) Quantitative bar plot for wall thickness.

(c) Dual immunofluorescence for α-SMA and PCNA showing smooth muscle pathology, scale 40 μm.

(d) Analysis of PCNA-positive cells. Data are mean ± SD, n = 8, analyzed by one-way ANOVA with Tukey post hoc. *P < 0.05, ***P < 0.001 vs control; ###P < 0.001 vs Su/Hx.

Ginsenoside Rg1 limits right ventricular hypertrophy in PH

Right ventricular structure and function were evaluated by small-animal echocardiography. Rats exposed to SuHx showed a sharp increase in RVAWT, demonstrating significant right ventricular hypertrophy **(Figures 3a and 3b)**. This abnormal increase was reduced following Rg1 treatment.

Consistent results were obtained with Fulton's index, which confirmed greater hypertrophy in hypoxia-exposed rats compared with normoxic controls but showed mitigation with Ginsenoside Rg1 **(Figure 3c)**.

Additionally, WGA staining revealed enlarged right ventricular cardiomyocytes in SuHx rats, whereas Rg1 administration reversed this increase in cell size **(Figures 3d and 3e)**.

Taken together, the data indicate that Ginsenoside Rg1 counteracts pathological right ventricular remodeling caused by combined SU5416 and hypoxia exposure.

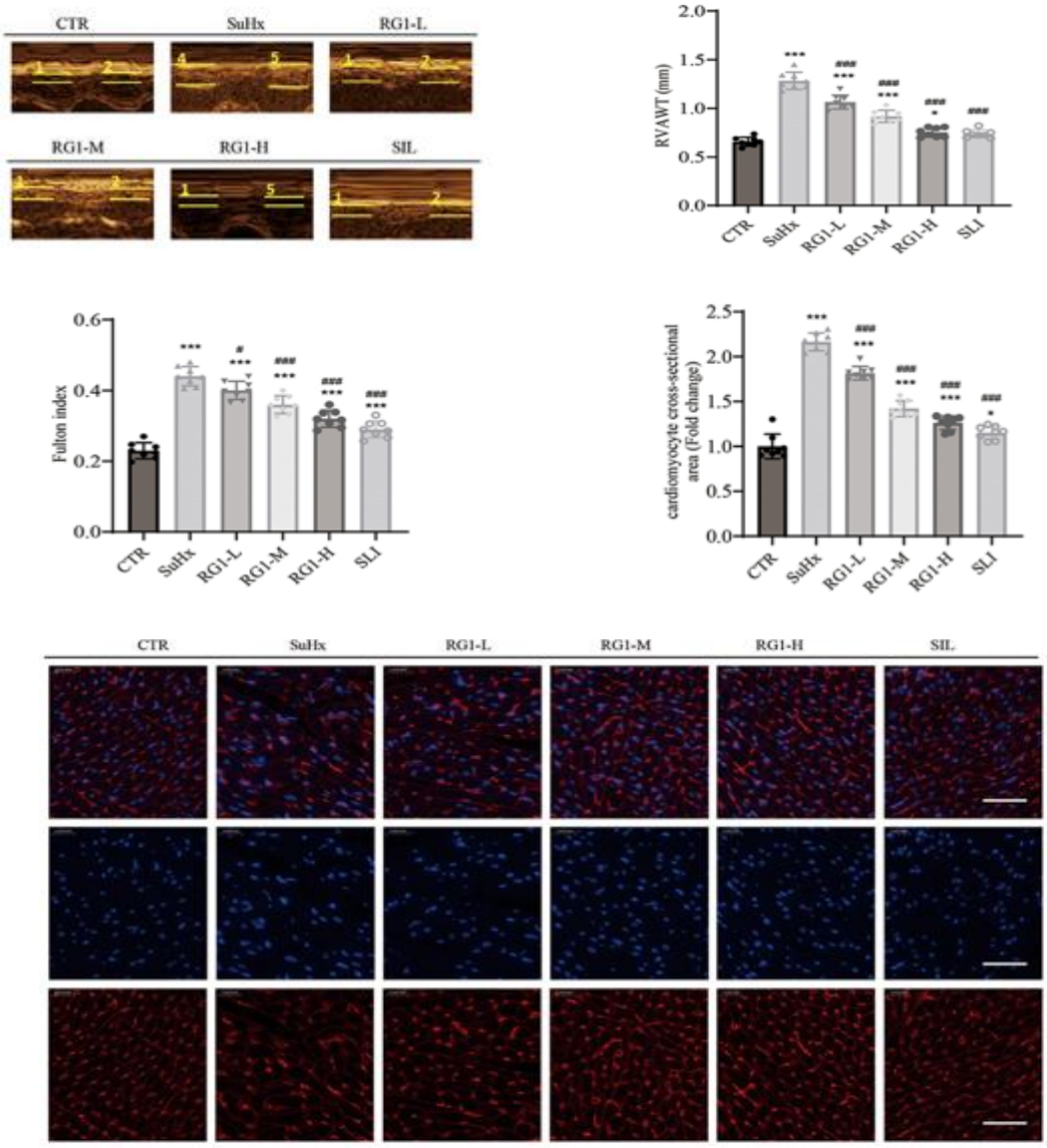

Figure 3. Ginsenoside Rg1 Improves Right Ventricular Structure and Function
(a) Representative images measuring RVAWT via echocardiography, scale 40 μm.
(b) Statistical representation of RVAWT.
(c) Fulton's index showing effects of Rg1 on ventricular hypertrophy.
(d–e) WGA-stained samples showing cardiomyocyte size and cross-sectional quantification, scale 40 μm.
Results shown as mean ± SD, n = 8, analyzed with one-way ANOVA and Tukey tests. *P < 0.05, ***P < 0.001 vs control; #P < 0.05, ###P < 0.001 vs Su/Hx.

Identification of molecular targets and functional pathway mapping

GeneCards and OMIM searches identified 9,525 PH-related differential genes. Predictive analysis using SwissTargetPrediction, SEA databases, and literature sources yielded 104 potential Ginsenoside Rg1 targets. Intersection of disease and compound target sets produced 92 shared genes **(Figure 4a)**.

A protein interaction map created using STRING and visualized in Cytoscape demonstrated 92 nodes and 730 edges. Based on degree ranking, the most prominent targets included IL6, AKT1, EGFR, SRC, STAT3, STING, NFKB1, PPARG, MMP9, IL2, and cGAS, designating them as key hubs involved in the Rg1–PH interaction network **(Figure 4b)**.

Functional characterization using the DAVID platform showed robust involvement of the HIF-1, FoxO, and cellular senescence pathways **(Figures 4c and 4d)**.

Molecular docking confirmed substantial binding potential between Ginsenoside Rg1 and cGAS **(Figure 4e)**. These results support the conclusion that cGAS-STING signaling, SASP regulation, and senescence-associated processes are major mechanistic axes through which Ginsenoside Rg1 exerts therapeutic effects in PH.

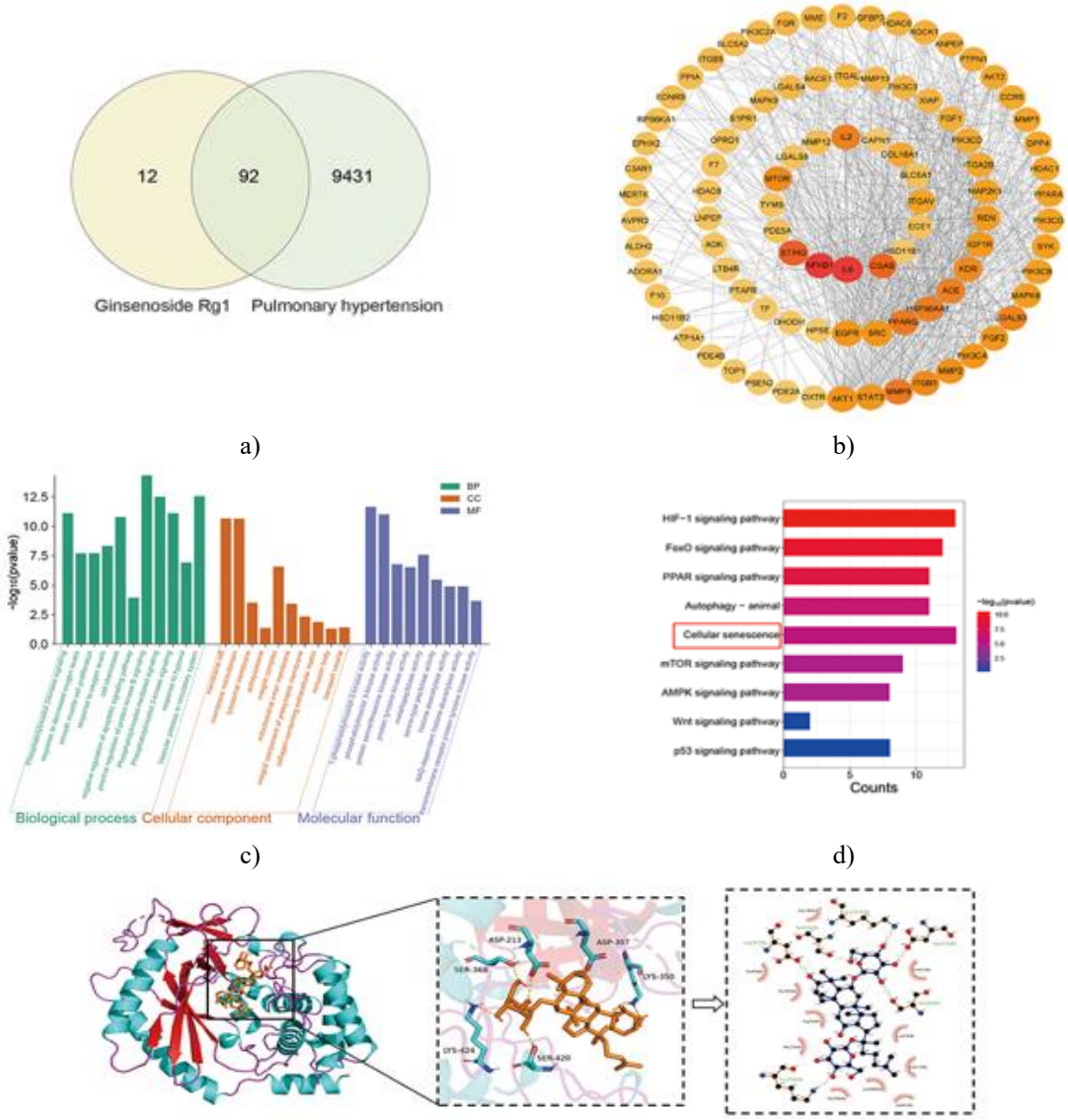

Figure 4. A systems-biology approach was applied to clarify how ginsenoside Rg1 may act in pulmonary hypertension.

(a) A Venn comparison was used to determine which molecular targets were jointly associated with both pulmonary hypertension and Rg1.

(b) The shared genes were then entered into a protein–protein interaction framework to highlight the most

influential molecular controllers.
(c) Gene Ontology enrichment outcomes.
(d) KEGG pathway enrichment results.
(e) Computer-aided docking illustrating the interaction between Rg1 and cGAS.

Ginsenoside Rg1 blocks cGAS/STING activation in vivo

To understand the pathways through which Rg1 protects against pulmonary hypertension, signaling components were examined in lung tissue derived from control and Sugen/hypoxia-exposed rats. Network and computational results indicated that the cGAS–STING axis might be a major target, and this was experimentally verified. In SuHx animals, both cGAS and STING mRNA were greatly increased, whereas Rg1 treatment strongly reduced these values **(Figures 5a and 5b)**.

Protein expression showed the same behavior. Western blots revealed that cGAS, STING, phosphorylated STING, TBK1, and phosphorylated TBK1 were markedly elevated in SuHx animals relative to controls, and administration of Rg1 clearly lowered all of these protein levels **(Figures 5c–5h)**. Immunofluorescent staining further showed intense cGAS and STING signals in pulmonary arteries after SuHx exposure, whereas these signals were substantially diminished following Rg1 treatment **(Figures 5i–5l)**. Thus, Rg1 effectively hinders the activation of the cGAS–STING pathway in the lungs of PH rats.

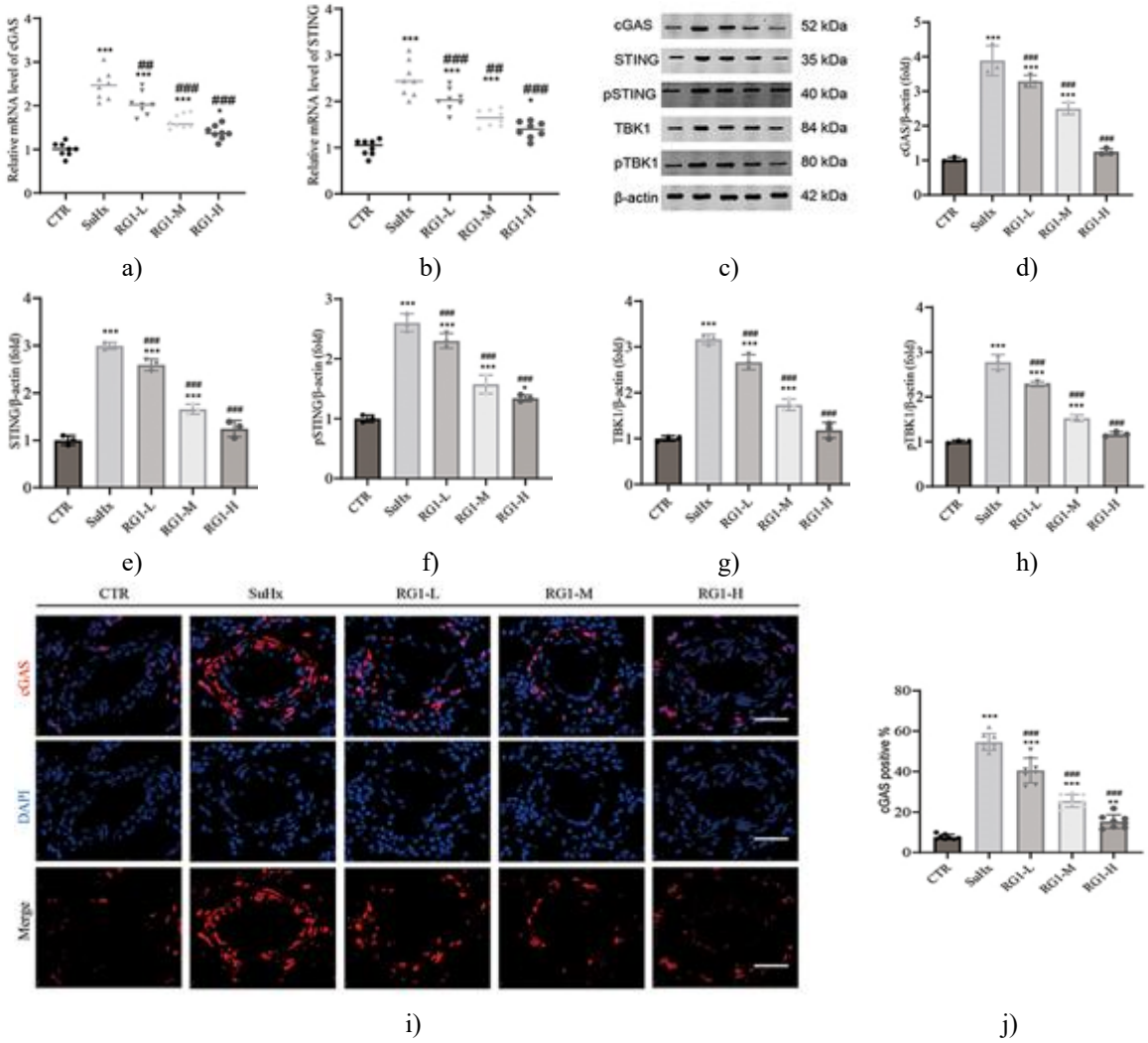

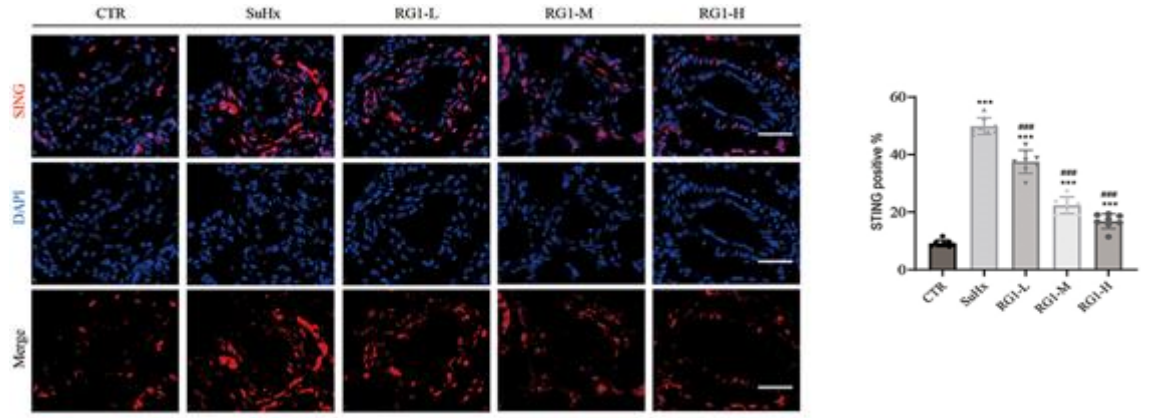

k) l)

Figure 5. Ginsenoside Rg1 decreases cGAS/STING pathway activation in the Su/Hx model.
(a–b) Relative transcript levels of cGAS and STING, n=8.
(c) Example Western blots showing cGAS, STING, p-STING, TBK1, and p-TBK1.
(d–h) Quantitative densitometry of the listed proteins, n=3.
(i) Imaging of cGAS staining, Scale bar = 40 μm.
(j) Quantification of cGAS-positive vascular cells, n=8.
(k) STING immunofluorescence, Scale bar = 40 μm.
(l) Quantification of STING-positive vascular cells, n=8. Data reported as mean ± SD. One-way ANOVA with Tukey testing. *P < 0.05, **P < 0.01, ***P < 0.001 vs control; ##P < 0.01, ###P < 0.001 vs Su/Hx.

Ginsenoside Rg1 reduces cellular aging and SASP activity in PH

To determine whether Rg1 influences senescence, the markers p16 and p21 were analyzed by RT-PCR, Western blotting, and immunohistochemistry. SuHx exposure substantially elevated the mRNA expression of both markers, but this increase was blunted when animals received Rg1 **(Figures 6a and 6b)**.

Protein data mirrored these results. SuHx led to strong induction of p16 and p21, while Rg1 minimized their expression **(Figures 6c–6e)**. Immunohistochemical staining confirmed consistent changes in lung sections **(Figures 6f–6i)**. These findings demonstrate that Rg1 counteracts PH-associated cellular senescence by downregulating major senescence markers.

SASP activity was also evaluated by measuring plasma NF-κB, IL-6, and IL-8 via ELISA **(Figures 7a–7c)**. All three inflammatory molecules were significantly reduced by Rg1 treatment, indicating suppression of SASP output in the SuHx model.

a) b)

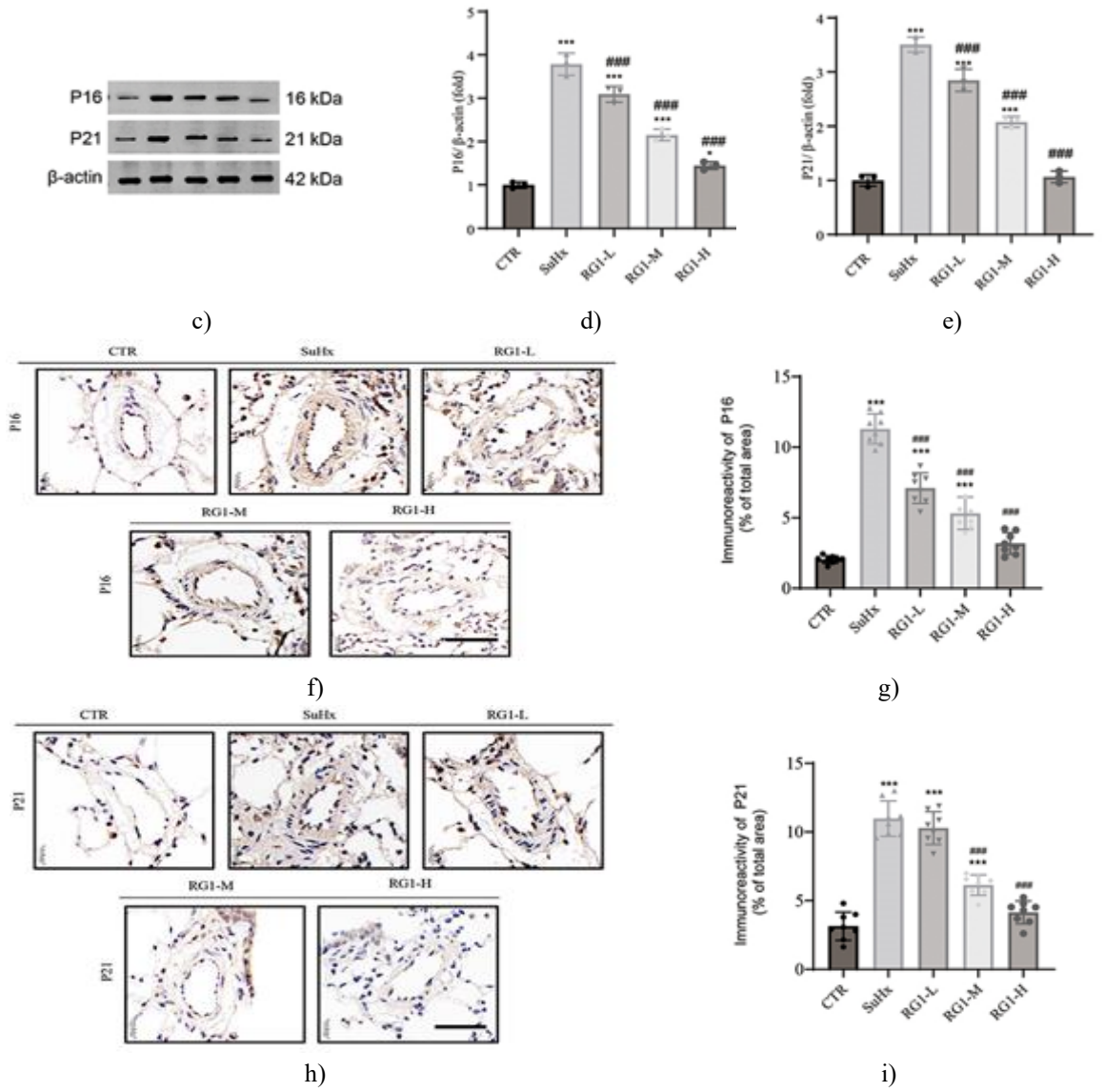

Figure 6. Ginsenoside Rg1 modifies senescence responses in pulmonary arterial tissue.
(a–b) p16 and p21 gene expression.
(c) Example Western blots of both markers.
(d–e) Quantified protein expression, n=3.
(f) Lung staining of p16, Scale bar = 40 μm.
(g) Quantification of p16-positive vascular cells, n=8.
(h) Lung staining of p21, Scale bar = 40 μm.
(i) Quantification of p21-positive vascular cells, n=8. Data reported as mean ± SD. One-way ANOVA with Tukey testing. *P < 0.05, ***P < 0.001 vs control; #P < 0.05, ##P < 0.01, ###P < 0.001 vs Su/Hx.

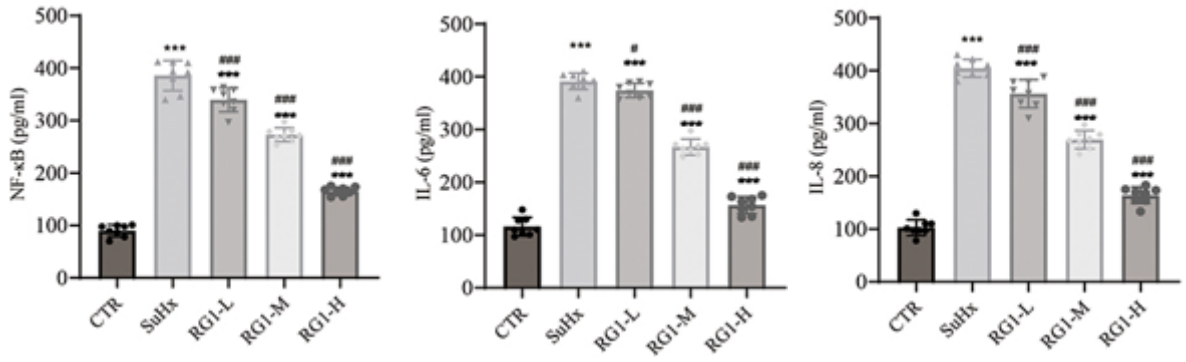

a) b) c)

Figure 7. Ginsenoside Rg1 reduces SASP activity in rats with PH.
(a) Circulating NF-κB concentrations in different experimental groups.
(b) Plasma IL-6 levels under the same conditions.
(c) Plasma IL-8 measurements across treatment groups. Values are expressed as mean ± SD, n=8. One-way ANOVA with Tukey post-test was applied. ***P < 0.001 vs control; #P < 0.05 and ###P < 0.001 vs Su/Hx.

Ginsenoside Rg1 demonstrates good tolerability in PH models

To determine whether Rg1 posed systemic toxicity, both blood indices and major organ function were examined. Body weight and complete blood count parameters did not show significant changes between Rg1-treated animals and controls (P>0.05, **(Figures 8a and 8b)**). Likewise, standard hepatic and renal biochemical markers (ALT, AST, BUN, Cr) showed no statistically meaningful differences among treatment groups (P>0.05, **(Figures 8c and 8d)**). HE-stained sections of liver, kidney, and spleen displayed normal morphology without detectable tissue injury **(Figures 8e–8g)**.

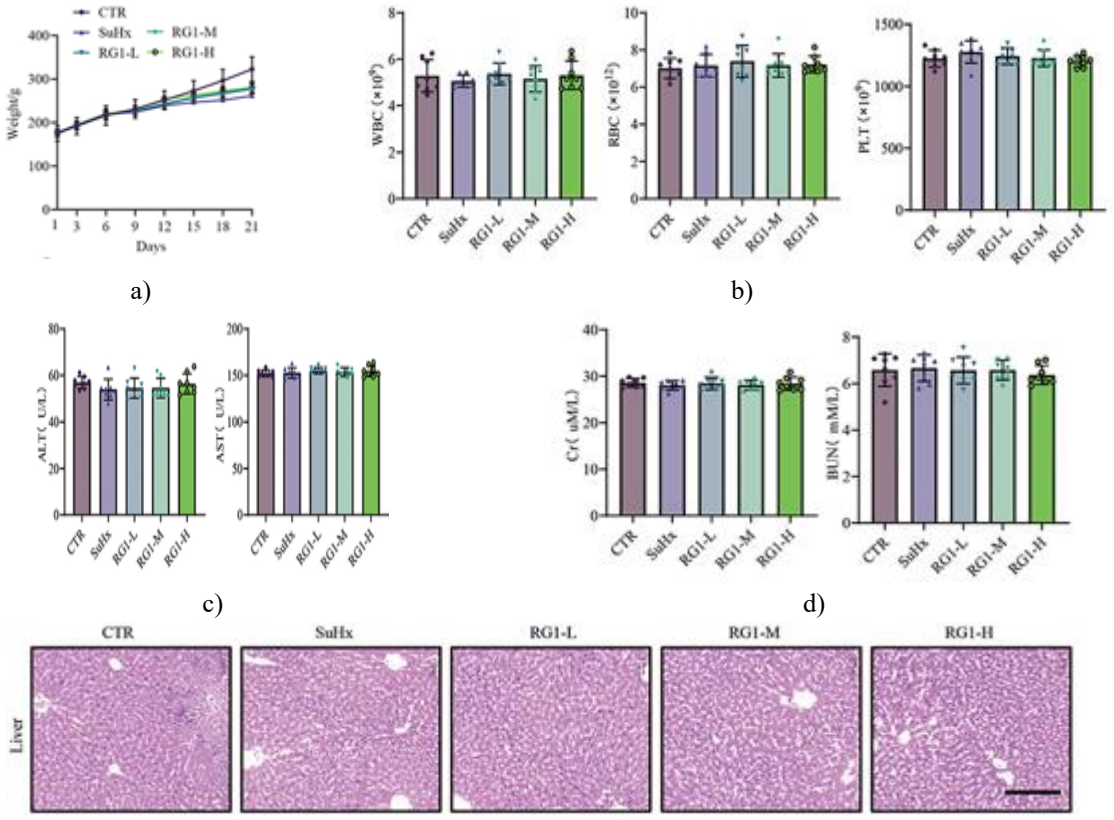

a) b) c) d) e)

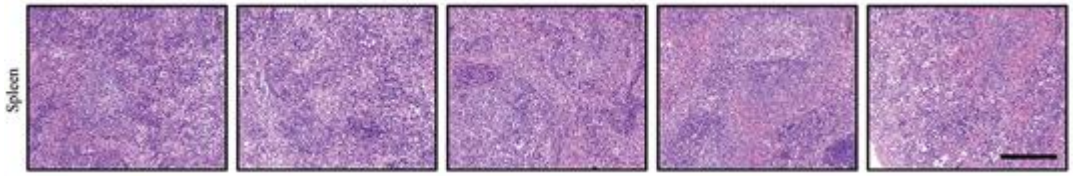

f)

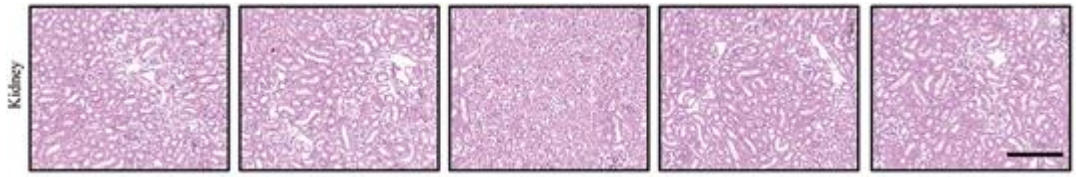

g)

Figure 8. In vivo evaluation of Rg1 safety.
(a) Rat body weight.
(b) Hematology profile including leukocytes, red cells, and platelets.
(c–d) Biochemical examination of ALT/AST and BUN/Cr.
(e–g) Histological examination of liver, spleen, and kidney using HE staining. Results shown as mean ± SD, n=8. One-way ANOVA with Tukey's test.

Pulmonary hypertension is a serious global disease with multifactorial causes and complex progression that complicates diagnosis and therapy. Numerous biological processes—including endothelial dysfunction, dysregulated smooth muscle proliferation, inflammation, and thrombosis—contribute to vascular structural remodeling, resulting in rising pulmonary vascular resistance and eventual right-sided heart impairment. Although the complete pathogenic sequence is still not fully understood, research indicates involvement of genetic alterations, epigenetic mechanisms, and environmental contributors. Many of these triggers accelerate abnormal cellular aging, and PH incidence and mortality are markedly higher in older individuals, highlighting the role of senescence as a central component of disease development.

Current PH medications—such as endothelin receptor blockers, PDE-5 inhibitors, prostacyclin analogs, and soluble guanylate cyclase stimulators—mainly act by modulating vascular tone and restraining proliferative responses. While they produce symptomatic benefit, they do not halt overall disease progression or reduce mortality, underscoring the need for novel therapeutic approaches that more directly target vascular remodeling. Cellular senescence represents a promising direction for such intervention.

Ginsenoside Rg1, one of the principal pharmacological compounds in ginseng, has been widely studied for its anti-aging capabilities. It reduces oxidative stress by decreasing ROS generation, lowering NOX2 expression, and raising SOD activity, helping protect mitochondrial integrity in degenerative conditions. In coronary artery disease, Rg1 enhances endothelial survival and limits oxidative injury and senescence through the AMPK/SIRT3/p53 cascade. Additionally, Rg1 promotes regenerative processes, supporting proliferation and repair of aging cells. It also inhibits hypoxia-induced inflammation, fibrosis, and aberrant cell proliferation by blocking the calpain-1/STAT3 pathway, contributing to reduced vascular remodeling. Another study demonstrated that Rg1 alleviates hypoxia-induced PH by increasing CCN1 expression, thereby suppressing TNF-α and IL-1β and limiting endothelial-to-mesenchymal transition. Although the therapeutic actions of Rg1 in PH have been documented, the extent to which its benefits depend on modulation of cellular aging has not been fully clarified.

In this work, a Sugen/hypoxia rat model of PH was established and confirmed using cardiac catheterization, echocardiography, and histological assessments. The model exhibited hallmark changes such as elevated RVSP, reduced TAPSE and PAT/PET, increased right ventricular cardiomyocyte size, and thickened arterial smooth muscle layers in small pulmonary vessels—consistent with known PH pathology. Using multiple concentrations of Rg1 in vivo, we demonstrated significant improvement in pulmonary pressures, enhanced right ventricular performance, and reduced vascular remodeling compared to untreated SuHx animals.

Mechanistic investigations showed that activation of the cGAS/STING pathway is linked with PVR in PH. Rg1 significantly downregulated this pathway at both mRNA and protein levels and decreased expression of the senescence markers p16 and p21 under hypoxic conditions. These results indicate that Rg1 improves pulmonary

vascular pathology by reducing senescence in a dose-dependent manner, supporting its potential as a pharmacological strategy for PH therapy.

The cGAS-STING pathway is widely recognized as a major initiator of cellular aging [34, 35]. In rodent models of PH induced by MCT, lung tissues exhibit markedly elevated expression of both cGAS and STING at the mRNA and protein levels [22, 23]. STING enhances vascular remodeling by activating the NLRP3 inflammasome within macrophages, thereby triggering inflammation and promoting abnormal cell growth in PH [36]. TBK1 acts as the critical kinase recruited by activated STING and regulates downstream interferon production and SASP signaling [37]. Phosphorylated TBK1 (pTBK1) drives cGAS/STING activation and contributes to chondrocyte aging, while TBK1 inhibition through BX795 blocks this pathway and reduces inflammatory and senescence-related activity in osteoarthritis [38]. In senescent cells, cytoplasmic chromatin fragments are sensed by cGAS, which activates cGAS–STING and stimulates strong SASP output, leading to paracrine propagation of senescence [39]. Senescent cells also release IL-6, a major SASP component, which interacts with its receptor to activate cytoplasmic DNA signaling pathways, further inducing cGAS-STING and NF-κB activation [40]. This series of events not only intensifies senescence in SASP-producing cells but also spreads senescence-promoting signals to adjacent cells, accelerating their proliferation and advancing widespread cellular aging. In the present study, ginsenoside Rg1 markedly decreased circulating SASP indicators, including NF-κB, IL-6, and IL-8, in SuHx-induced PH rats, offering new mechanistic evidence for the beneficial effects of Rg1 and underscoring the central contribution of cGAS/STING to the senescence process.

To strengthen evidence for the anti-PH mechanisms of ginsenoside Rg1, further experiments will be conducted in vitro using primary PASMCs under hypoxic stimuli. The activity of the cGAS/STING pathway will be modified using siRNA knockdown strategies and specific pharmacological activators or inhibitors to directly assess the effects of Rg1 on senescence-related proteins and downstream molecular targets. Additionally, dose-optimization studies will be performed to determine a long-term effective treatment regimen, and translational value will be explored in multiple species through detailed pharmacokinetics and biomarker assessment. This comprehensive research plan is expected to speed the development of ginsenoside Rg1 from early mechanistic studies toward a novel therapeutic candidate for PH.

Conclusion

In summary, this research confirms that ginsenoside Rg1 alleviates vascular remodeling in a PH model produced through Sugen exposure combined with hypoxia. Rg1 suppressed cGAS-STING activation in Su/Hx rats, thereby reducing SASP production and limiting cellular senescence. These results clarify how ginsenoside Rg1 mitigates vascular pathology through inhibition of cGAS-STING signaling and senescence, supporting its therapeutic potential as a naturally derived agent for conditions associated with aging.

Acknowledgments: None

Conflict of Interest: None

Financial Support: None

Ethics Statement: None

References

1. Mocumbi A, Humbert M, Saxena A, Jing ZC, Sliwa K, Thienemann F, et al. Pulmonary hypertension. Nat Rev Dis Prim. 2024;10(1):1. doi:10.1038/s41572-023-00486-7
2. Chin KM, Gaine SP, Gerges C, Jing ZC, Mathai SC, Tamura Y, et al. Treatment algorithm for pulmonary arterial hypertension. Europ Resp J. 2024;64(4). doi:10.1183/13993003.01325-2024
3. Fukumoto Y. Pathophysiology and treatment of pulmonary arterial hypertension. Int J Mol Sci. 2024;25(2). doi:10.3390/ijms25021166
4. Li X, Tan J, Wan J, Cheng B, Wang YH, Dai A. Cell death in pulmonary arterial hypertension. Int J Med Sci. 2024;21(10):1840–51. doi:10.7150/ijms.93902

5. Shlobin OA, Adir Y, Barbera JA, Cottin V, Harari S, Jutant EM, et al. Pulmonary hypertension associated with lung diseases. Europ Resp J. 2024;64(4). doi:10.1183/13993003.01200-2024
6. Kovacs G, Bartolome S, Denton CP, Gatzoulis MA, Gu S, Khanna D, et al. Definition, classification and diagnosis of pulmonary hypertension. Europ Resp J. 2024;64(4). doi:10.1183/13993003.01324-2024
7. de Magalhães JP. Cellular senescence in normal physiology. Science. 2024;384(6702):1300–1. doi:10.1126/science.adj7050
8. Dierick JF, Eliaers F, Remacle J, Raes M, Fey SJ, Larsen PM, et al. Stress-induced premature senescence and replicative senescence are different phenotypes, proteomic evidence. Biochem Pharmacol. 2002;64(5–6):1011–7. doi:10.1016/s0006-2952(02)01171-1
9. Reimann M, Lee S, Schmitt CA. Cellular senescence: neither irreversible nor reversible. J Exp Med. 2024;221(4). doi:10.1084/jem.20232136
10. Volonte D, Benson CJ, Daugherty SL, Beckel JM, Trebak M, Galbiati F. Purinergic signaling promotes premature senescence. J Biol Chem. 2024;300(4):107145. doi:10.1016/j.jbc.2024.107145
11. Qin T, Chen T, Ma R, Li H, Li C, Zhao J, et al. Stress hormones: unveiling the role in accelerated cellular senescence. Aging Dis. 2024. doi:10.14336/ad.2024.0262
12. Lazzarini E, Lodrini AM, Arici M, Bolis S, Vagni S, Panella S, et al. Stress-induced premature senescence is associated with a prolonged QT interval and recapitulates features of cardiac aging. Theranostics. 2022;12(11):5237–57. doi:10.7150/thno.70884
13. Liu L, Wei Y, Giunta S, He Q, Xia S. Potential role of cellular senescence in pulmonary arterial hypertension. Clin Exp Pharmacol Physiol. 2022;49(10):1042–9. doi:10.1111/1440-1681.13696
14. Safaie Qamsari E, Stewart DJ. Cellular senescence in the pathogenesis of pulmonary arterial hypertension: the good, the bad and the uncertain. Front Immunol. 2024;15:1403669. doi:10.3389/fimmu.2024.1403669
15. Wang B, Han J, Elisseeff JH, Demaria M. The senescence-associated secretory phenotype and its physiological and pathological implications. Nat Rev Mol Cell Biol. 2024;25(12):958–78. doi:10.1038/s41580-024-00727-x
16. Van Der Feen DE, Bossers GP, Hagdorn QA, Moonen JR, Kurakula K, Szulcek R, et al. Cellular senescence impairs the reversibility of pulmonary arterial hypertension. Sci Trans Med. 2020;12(554). doi:10.1126/scitranslmed.aaw4974
17. Dvorkin S, Cambier S, Volkman HE, Stetson DB. New frontiers in the cGAS-STING intracellular DNA-sensing pathway. Immunity. 2024;57(4):718–30. doi:10.1016/j.immuni.2024.02.019
18. Zhang Q, Shen L, Ruan H, Huang Z. cGAS-STING signaling in cardiovascular diseases. Front Immunol. 2024;15:1402817. doi:10.3389/fimmu.2024.1402817
19. Yu L, Liu P. cGAS/STING signalling pathway in senescence and oncogenesis. Semi Cancer Biol. 2024;106-107:87–102. doi:10.1016/j.semcancer.2024.08.007
20. Wei M, Li Q, Li S, Wang D, Wang Y. Multifaceted roles of cGAS-STING pathway in the lung cancer: from mechanisms to translation. PeerJ. 2024;12:e18559. doi:10.7717/peerj.18559
21. Feng Q, Xu X, Zhang S. cGAS-STING pathway in systemic lupus erythematosus: biological implications and therapeutic opportunities. Immunol Res. 2024;72(6):1207–16. doi:10.1007/s12026-024-09525-1
22. Yan X, Huang J, Zeng Y, Zhong X, Fu Y, Xiao H, et al. CGRP attenuates pulmonary vascular remodeling by inhibiting the cGAS-STING-NFκB pathway in pulmonary arterial hypertension. Biochem Pharmacol. 2024;222:116093. doi:10.1016/j.bcp.2024.116093
23. Li J, Meng ZY, Wen H, Lu CH, Qin Y, Xie YM, et al. β-sitosterol alleviates pulmonary arterial hypertension by altering smooth muscle cell phenotype and DNA damage/cGAS/STING signaling. Phytomedicine. 2024;135:156030. doi:10.1016/j.phymed.2024.156030
24. Ito H, Ito M. Recent trends in ginseng research. J Nat Med. 2024;78(3):455–66. doi:10.1007/s11418-024-01792-4
25. Fan W, Fan L, Wang Z, Mei Y, Liu L, Li L, et al. Rare ginsenosides: a unique perspective of ginseng research. J Adv Res. 2024;66:303–28. doi:10.1016/j.jare.2024.01.003
26. Ratan ZA, Youn SH, Kwak YS, et al. Adaptogenic effects of panax ginseng on modulation of immune functions. J Ginseng Res. 2021;45(1):32–40. doi:10.1016/j.jgr.2020.09.004
27. Zhou G, Wang CZ, Mohammadi S, Sawadogo WR, Ma Q, Yuan CS. Pharmacological effects of ginseng: multiple constituents and multiple actions on humans. Am J Chin Med. 2023;51(5):1085–104. doi:10.1142/s0192415x23500507

28. Shi M, Ma J, Jin S, Wang T, Sui Y, Chen L. Effects of saponins Rb(1) and re in American ginseng combined intervention on immune system of aging model. Front Mol Biosci. 2024;11:1392868. doi:10.3389/fmolb.2024.1392868
29. Lin LQ, Mao FK, Lin J, Guo L, Yuan WR, Wang BY. Ginsenoside Rg1 induces ferroptosis by regulating the focal adhesion kinase/protein kinase B-forkhead box O3A signaling pathway and alleviates sepsis-induced myocardial damage. J Physiol Pharmacol. 2024;75(4). doi:10.26402/jpp.2024.4.04
30. Wu Z, Huang J, Bai X, Wang Q, Wang F, Xu J, et al. Ginsenoside-Rg1 mitigates cardiac arrest-induced cognitive damage by modulating neuroinflammation and hippocampal plasticity. Eur J Pharmacol. 2023;938:175431. doi:10.1016/j.ejphar.2022.175431
31. Huang C, Xue X, Gong N, Jiang J. Ginsenoside Rg1 suppresses paraquat-induced epithelial cell senescence by enhancing autophagy in an ATG12-dependent manner. Environ Toxicol. 2022;37(9):2302–13. doi:10.1002/tox.23597
32. Tang BL, Liu Y, Zhang JL, Lu ML, Wang HX. Ginsenoside Rg1 ameliorates hypoxia-induced pulmonary arterial hypertension by inhibiting endothelial-to-mesenchymal transition and inflammation by regulating CCN1. Biomed Pharmacothe. 2023;164:114920. doi:10.1016/j.biopha.2023.114920
33. National Research Council Committee for the Update of the Guide for the C, Use of Laboratory A. The National Academies Collection: reports funded by National Institutes of Health. In: Guide for the Care and Use of Laboratory Animals. National Academies Press (US) Copyright © 2011, National Academy of Sciences; 2011.
34. Loo TM, Miyata K, Tanaka Y, Takahashi A. Cellular senescence and senescence-associated secretory phenotype via the cGAS-STING signaling pathway in cancer. Cancer Sci. 2020;111(2):304–11. doi:10.1111/cas.14266
35. Wu Q, Leng X, Zhang Q, Zhu YZ, Zhou R, Liu Y, et al. IRF3 activates RB to authorize cGAS-STING-induced senescence and mitigate liver fibrosis. Sci Adv. 2024;10(9):eadj2102. doi:10.1126/sciadv.adj2102
36. Wu DD, Deng Y, Liao J, Xie SS, Meng H, Lan WF. STING mediates SU5416/hypoxia-induced pulmonary arterial hypertension in rats by regulating macrophage NLRP3 inflammasome activation. Immunobiology. 2023;228(2):152345. doi:10.1016/j.imbio.2023.152345
37. Zhang D, Liu Y, Zhu Y, Zhang Q, Guan H, Liu S, et al. A non-canonical cGAS-STING-PERK pathway facilitates the translational program critical for senescence and organ fibrosis. Nat Cell Biol. 2022;24(5):766–82. doi:10.1038/s41556-022-00894-z
38. Lu R, Qu Y, Wang Z, He Z, Xu S, Cheng P, et al. TBK1 pharmacological inhibition mitigates osteoarthritis through attenuating inflammation and cellular senescence in chondrocytes. J Orthopaedic Translation. 2024;47:207–22. doi:10.1016/j.jot.2024.06.001
39. Glück S, Guey B, Gulen MF, Wolter K, Kang TW, Schmacke NA, et al. Innate immune sensing of cytosolic chromatin fragments through cGAS promotes senescence. Nat Cell Biol. 2017;19(9):1061–70. doi:10.1038/ncb3586
40. Herbstein F, Sapochnik M, Attorresi A, Pollak C, Senin S, Gonilski-Pacin D, et al. The SASP factor IL-6 sustains cell-autonomous senescent cells via a cGAS-STING-NFκB intracrine senescent noncanonical pathway. Aging Cell. 2024;23(10):e14258. doi:10.1111/acel.14258